

An Extension of the Worm Like Chain Model Appropriate to Double-Strand DNA Subject to Spatial Constraints

C. Bouchiat

*Laboratoire de Physique Théorique de l'Ecole Normale Supérieure
24, rue Lhomond, F-75231 Paris Cedex 05, France.*

(Dated: December 2, 2024)

In absence of supercoiling, the Worm Like Chain (WLC) model provides a good description of the entropic elasticity within a wide range of force. Since the elastic-energy linear density of the WLC model is proportional to the inverse square of the molecular chain curvature radius, a natural dynamical variable is the unitary tangent vector to the chain but this choice leads to unbearable complications if one wishes to implement spatial constraints via a one-monomer potential. To circumvent this difficulty the first obvious step is to use the monomer coordinate as a dynamical variable. If it were used as the sole dynamical variable, second-order derivatives with respect to the chain arc length would creep in the elastic energy. This can be avoided by introducing an auxiliary vector variable. Running the usual theoretical machinery, we arrive to a remarkably simple extension of the WLC (EWLC) model, where both the monomer coordinate and the tangent vector appear as independent variable. We have found that a formulation of the EWLC model, based upon the “transfer matrix” method, has a nice interpretation in terms of a Markovian random walk in three dimensions and is numerically rather efficient. The model is then defined by writing the recurrence relation connecting the probability distributions of the dynamical variables relative to adjacent monomers along the discretized chain. Each step involves a coordinate translation along a direction correlated to that of the previous one, together with an energy exchange with the thermal bath governed by the Boltzmann factor associated with the one-monomer potential. As an illustration, we have studied two configurations of a single dsDNA molecule confined between two parallel plates. One molecule end is anchored to the first plate by a biochemical bond. A stretching force, normal to the plates, is pulling the other end away from the anchoring plate. In the first case the crystallographic length is smaller than the two-plate distance. The molecule feels then only the anchoring barrier effect. As expected, the predicted elongation-versus-force curve is pushed upward with respect to the WLC model result. In the second case, the crystallographic length can take values as large as $3/2$ the two-plate distance, with a stretching force such that the molecule elongated according to the WLC model would not fit between the two plates. The molecule manages to squeeze into the plates, when its variable crystallographic length approaches its maximum value, by following around the symmetry axis a zigzagging path, which becomes gradually parallel to the plates. We end the paper by two suggestions: the first one is a generalization of the EWLC model to supercoiled dsDNA, the second one is the study of a dsDNA chain interacting with a stochastic imaginary one-monomer potential, as a possible approach to self-avoidance.

PACS numbers: 87.15.By, 61.41+e

Introduction

In the last ten years Single Molecule Biophysics has become a very active field of research. Among the recently explored areas, one finds the observation, at the one-molecule level, of the biochemical interactions of the double strand DNA (dsDNA) with the various proteins involved in the duplication process (for two recent reviews see, for instance, the references [1, 2]). The protein-DNA interaction is detected by the observation, in real time, of the variations of the dsDNA elongation under the action of a fixed stretching force. It was clearly of interest to have a good physical understanding of the dsDNA elasticity measurements [3, 4, 5]. In absence of DNA supercoiling, this is provided by the so called “Worm Like Chain Model” (WLC) [6, 7, 8] which gives a good description of the dsDNA entropic bending elasticity within a wide range of force, from few hundredths to few tens of picoNewton.

In practice, the persistence length of a double helix

is about five times the typical length resolution. It is, then, legitimate to use a rectifiable curve to represent the coarse-grained dsDNA chain. The basic hypothesis of the WLC model is to assume that the elastic-energy linear density is proportional to the inverse square of the chain curvature radius. In the usual formulation of the WLC model, the relevant Statistical Mechanics variable is the tangent vector $\mathbf{t}(s) = d\mathbf{r}/ds$ where $\mathbf{r}(s)$ is the effective monomer coordinate and ds the rectifiable chain length element. The elastic molecular-chain energy is given, in thermal units $k_B T$, by the following line integral:

$$E_{WLC} = \int_0^L ds \left(\frac{A}{2} \left(\frac{d\mathbf{t}(s)}{ds} \right)^2 - \mathbf{f} \cdot \mathbf{t}(s) \right), \quad (1)$$

where L is the crystallographic length of the polymer. A is the persistence length and $(d\mathbf{t}(s)/ds)^2$ is the inverse square of the curvature radius of the coarse-grained chain. $\mathbf{F} = k_B T \mathbf{f}$ stands for the stretching force, applied to the extremity of the chain. It follows from its very definition that \mathbf{t} is a unit vector. The partition function Z

is given by the functional Boltzman integral:

$$Z = \int \mathcal{D}[\theta] \mathcal{D}[\phi] \exp -E_{WLC}, \quad (2)$$

where the integration has to be performed over the paths drawn upon the unit sphere. This problem can be mapped onto a well-defined Quantum Mechanics problem, namely, the precession, in a d.c. electric field, of a diatomic molecule endowed with a permanent electric dipole moment. The associated differential equation, with specific boundary conditions, has been solved with a very good precision in ref.[8].

However, this approach becomes awkward if one wishes to impose physical constraints involving the monomer space coordinate. For instance, one may wish to confine the molecule in a certain region of space. This constraint can be formulated in terms of a potential, $V(\mathbf{r}(s))$, acting on each monomer of coordinate $\mathbf{r}(s)$. If the tangent vector $\mathbf{t}(s)$ is the sole dynamical variable, one has to write $\mathbf{r}(s) = \int_0^s \mathbf{t}(s')ds'$ and the potential energy to be added to E_{WLC} has the ugly non-local form:

$$\Delta E_{WLC}^{pot} = \int_0^L ds V \left(\int_0^s \mathbf{t}(s')ds' \right). \quad (3)$$

This situation becomes worse if one studies self-avoiding effects described by a monomer-monomer repulsive potential, $V(\mathbf{r}(s_1), \mathbf{r}(s_2))$:

$$\Delta E_{WLC}^{SA} = \int_0^L ds_1 \int_0^L ds_2 V \left(\int_0^{s_1} \mathbf{t}(s'_1)ds'_1, \int_0^{s_2} \mathbf{t}(s'_2)ds'_2 \right). \quad (4)$$

We indicate now the organization of the paper.

The first obvious step to avoid the above ugly expressions for the monomer potential energy is to use the monomer coordinate $\mathbf{r}(s)$ as a dynamical variable. We shall develop our whole procedure for a family of polymer models defined by the elastic-energy linear density: $\mathcal{E}(s) = \mathcal{E}_0(\dot{\mathbf{r}}^2) + \frac{1}{2} A \ddot{\mathbf{r}}^2 - \mathbf{f} \dot{\mathbf{r}} + V(\mathbf{r})$. *A priori*, our first move does not look like a very clever one, since we have introduced second-order derivatives in the elastic energy, via the curvature term $\frac{1}{2} A \ddot{\mathbf{r}}^2$. The mapping onto a Quantum Mechanics problem is no longer as evident as it was in reference[8].

Our second step will be to eliminate all second-order derivatives at the price of introducing in the elastic energy an auxiliary dynamical variable $\mathbf{u}(s)$, using a simple identity involving Gaussian integrals. (Section 1)

We will then be able to run the usual machinery to build the transfer matrix and the associated Hamiltonian operator \hat{H} , starting from the discretized functional integral giving the partition function. (Section 2.1) We will clarify in Section 2.2 the physical interpretation of the auxiliary variable \mathbf{u} , which is defined up to a multiplicative constant λ . With an appropriate choice of λ , its conjugate momentum \mathbf{p}_u is identified to the “velocity” operator $\hat{\mathbf{v}} = [\hat{H}, \mathbf{r}]$. The Hamiltonian operator \hat{H} , written in a basis diagonal with respect to $\hat{\mathbf{v}}$, has a

remarkably simple form, involving mathematical objects with well defined physical interpretations (Section 2.2).

At this point, it is a rather easy task to get the Hamiltonian operator for an extended WLC model, allowing for spatial constraints : one chooses $\mathcal{E}_0(\mathbf{v}^2) = b(\mathbf{v}^2 - 1)^2/(2\delta b^2)$ and takes the limit $\delta b/b \ll 1$ where \mathbf{v} can be identified to the unitary vector \mathbf{t} of the WLC model. The tangent vector is reappearing as a dynamical variable under a somewhat disguised form, but this time, in association with the monomer coordinate. The end result will turn out to be a rather transparent relation between our Extended WLC (EWLC) model Hamiltonian and the the unconstrained WLC model:

$$\hat{H}_{EWLC} = \hat{H}_{WLC}(\mathbf{f}) + \mathbf{t} \cdot \nabla_{\mathbf{r}} + V(\mathbf{r}).$$

Instead of trying to get the entropic elasticity, as in ref.[8] by solving the eigenvalue problem associated with the differential operator \hat{H}_{EWLC} , we shall follow in Section 3 a more leisurely route: namely an iterative construction of the partition function via the transfer matrix formalism. We shall derive, from the transfer operator $\hat{T} = \exp -b \hat{H}_{EWLC}$, a recurrence relation involving the n^{th} -order partition function $Z_n(\mathbf{r}_n, \mathbf{t}_n)$, which gives the probability distribution of the variables \mathbf{r}_n and \mathbf{t}_n , relative to the n^{th} effective monomer:

$$Z_{n+1}(\mathbf{r}_{n+1}, \mathbf{t}_{n+1}) = \exp -b V(\mathbf{r}_{n+1}) \times \int d^3 \mathbf{t}_n \langle \mathbf{t}_{n+1} | \hat{T}_{WLC}(\mathbf{f}) | \mathbf{t}_n \rangle Z_n(\mathbf{r}_{n+1} - b \mathbf{t}_{n+1}, \mathbf{t}_n),$$

where $\hat{T}_{WLC}(\mathbf{f})$ is the transfer operator of the unconstrained WLC model. A rather evident connection with a Markovian random walk in three dimensions will be explicated.

The last two sections will be devoted to some illustrations of the formalism presented in this paper. Our testing ground will be the study of the entropic elasticity of a single dsDNA molecule confined between two parallel plates. One molecule end is anchored to one plate by a biochemical binding. A stretching force, normal to the plates, is pulling away the free molecular end from the anchoring plate. For the sake of simplicity, we shall ignore, in this illustrative analysis, the spatial obstructions associated with the stretching devices (magnetic and optical tweezers ...). Two configurations will be studied.

In the first one, the cristallographic length L is supposed to be larger than the two-plate distance L_0 , so that the entropic elasticity is affected only by the anchoring plate barrier. For a relatively short molecule ($L/A = 12$), we will compute the elongation-versus-force curve, which is expected to be pushed upward with respect to the unconstrained WLC model predictions, notably for the zero-force case. There is a very simple qualitative explanation: taking the z -axis normal to the plate and directed along the force, the half space $z < 0$ is not accessible to the momomers whatever the force.

The second configuration corresponds to a confined situation where the cristallographic length L and the two-plate distance L_0 are in the ratio 3 to 2. If one takes

the value $\alpha = FA/(k_B T) = 5$ for the reduced force parameter, the molecule stretched according to the unconstrained WLC model could not fit inside the plates. We will investigate how a molecule of variable length manages to satisfy the two-plate constraints. When L approaches $3/2 L_0$, we shall find that the molecule end follows around the symmetry axis a zigzagging path which becomes gradually parallel to the plates.

In the concluding remarks, we shall suggest, among others, two possible applications of our theoretical approach to the study of "stiff" polymers.

It is a relatively trivial matter to generalize our extended version of the WLC model to the transfer matrix formulation of the RLC model [11], which incorporates both bending and twisting rigidities. The anchoring barrier effects are expected to be significant when the reduced supercoiling parameter σ is above the threshold -at fixed force- for the creation of plectonem configurations, since the stretching force potential energy vanishes for such structures.

It is well known that the polymer self-avoidance problem, induced by a two-monomer repulsive potential $V(\mathbf{r}_1, \mathbf{r}_2)$ can be mapped into that of a polymer interacting with a one-monomer imaginary stochastic potential $i\phi(\mathbf{r})$, having a Gaussian probability measure such that $\langle\phi(\mathbf{r}_1, \phi(\mathbf{r}_2))\rangle_\phi = V(\mathbf{r}_1, \mathbf{r}_2)$. Our formulation of the WLC (and RLC) model, which allows for the incorporation of a one-monomer potential energy in a simple way, suggests that the self-avoidance problem for "stiff" polymers might be amenable to Quantum Field Theory Techniques. This approach looks untractable within the standard formulation of the WLC (and RLC) models.

I. THE ELIMINATION OF SECOND-ORDER DERIVATIVES IN THE ELASTIC ENERGY WITH THE HELP OF AN AUXILIARY VARIABLE.

We would like to explore first the possibility of using the monomer coordinate $\mathbf{r}(s)$, as the sole dynamical variable, allowing for the presence of the monomer coordinate $\mathbf{r}(s)$ second-order derivative in the elastic-energy linear density. More precisely, we are going to study the statistical properties of the class of polymer models, defined by the following partition function:

$$Z = \int \mathcal{D}[\mathbf{r}] \exp \left(- \int_0^L \mathcal{E}(s) ds \right), \quad (5)$$

$$\mathcal{E}(s) = \mathcal{E}_0(\ddot{\mathbf{r}}^2) + \frac{1}{2} A \ddot{\mathbf{r}}^2 - \mathbf{f} \cdot \dot{\mathbf{r}} + V(\mathbf{r}), \quad (6)$$

with $\dot{\mathbf{r}} = \frac{d\mathbf{r}}{ds}$ and $\ddot{\mathbf{r}} = \frac{d^2\mathbf{r}}{ds^2}$. It should be stressed that the variable s with $0 \leq s \leq L$ results from a coarse graining of the molecular chain. We shall see later on that for suitable choice of $\mathcal{E}_0(\ddot{\mathbf{r}}^2)$ the variable coincides, to an arbitrary precision, with the arc-length s appearing in the WLC model.

To compute the partition function we have to resort to a discretization of the variable s : $s_n = n b$. The molecular chain is then represented by N elementary links or effective monomers with $N = L/b$. Assuming that the effective monomer length b is much smaller than the characteristic length A , we can write:

$$\dot{\mathbf{r}} = \frac{\mathbf{r}_{n+1} - \mathbf{r}_n}{b}, \quad \ddot{\mathbf{r}} = \frac{\mathbf{r}_{n+1} - 2\mathbf{r}_n + \mathbf{r}_{n-1}}{b^2}. \quad (7)$$

The partition function is then given as an integral of a product of $N - 1$ monomer coordinate \mathbf{r}_n functions:

$$Z = \int \prod_{n=1}^{N-1} d^2 \mathbf{r}_n \exp -b \left(\mathcal{E}_0(\mathbf{r}_n^2) + \frac{1}{2} A \ddot{\mathbf{r}}_n^2 - \mathbf{f} \cdot \dot{\mathbf{r}}_n + V(\mathbf{r}_n) \right). \quad (8)$$

We are going to use a mathematical trick to eliminate the $\ddot{\mathbf{r}}^2$ terms at the price of introducing an auxiliary dynamical variable \mathbf{u} . The starting point is the integral identity, written for fixed n :

$$\exp -\frac{A}{2}(\ddot{\mathbf{r}}_n)^2 \equiv C(A)^{-1} \times \int_{-\infty}^{\infty} d^3 \mathbf{u}_n \exp -A/2 ((\lambda \mathbf{u}_n + i \ddot{\mathbf{r}}_n)^2 + \ddot{\mathbf{r}}_n^2). \quad (9)$$

The constant λ is a kind of gauge constant, in the sense that all physical results are independent of its value provided that the condition $\Re(\lambda) > \Im(\lambda)$ is satisfied in order to guarantee that the integral $\int_{-\infty}^{+\infty} d^3 \mathbf{u}_n \exp -A/2 (\lambda \mathbf{u}_n + i \ddot{\mathbf{r}}_n)^2$ converges to the value $C(A) = \left(\frac{2\pi}{\lambda A}\right)^{\frac{3}{2}}$. Expanding the argument of the exponential we get the final identity:

$$\exp -\frac{A}{2}(\ddot{\mathbf{r}}_n)^2 \equiv \int_{-\infty}^{+\infty} d^3 \mathbf{u}_n \exp -A \left(\frac{1}{2} \mathbf{u}_n^2 + i \lambda \mathbf{u}_n \cdot \ddot{\mathbf{r}}_n \right). \quad (10)$$

We arrive in this way to an expression of $\mathcal{E}(s)$ involving now the two variables \mathbf{r} and \mathbf{u} :

$$\mathcal{E}(s) \rightarrow \mathcal{E}_0(\dot{\mathbf{r}}^2) + i A \lambda \mathbf{u} \cdot \ddot{\mathbf{r}} + A \frac{\lambda^2}{2} \mathbf{u}^2 - \mathbf{f} \cdot \dot{\mathbf{r}} + V(\mathbf{r}). \quad (11)$$

Let us perform the following integration by part:

$$\int_0^L ds \mathbf{u} \cdot \ddot{\mathbf{r}} = [\mathbf{u} \cdot \dot{\mathbf{r}}]_0^L - \int_0^L ds (\dot{\mathbf{r}} \cdot \dot{\mathbf{u}}). \quad (12)$$

Forgetting the "surface terms" [15], we get the new expression of the elastic-energy density:

$$\mathcal{E}_{new}(\mathbf{r}, \dot{\mathbf{r}}, \mathbf{u}, \dot{\mathbf{u}}) = \mathcal{E}_0(\dot{\mathbf{r}}^2) - i A \lambda \dot{\mathbf{u}} \cdot \dot{\mathbf{r}} - \mathbf{f} \cdot \dot{\mathbf{r}} + V(\mathbf{r}) + A \frac{\lambda^2}{2} \mathbf{u}^2. \quad (13)$$

We have now a "kinetic term", which depends only upon *first-order derivatives*, so that we can use the Lagrange-Hamilton formalism.

It is of interest to get the equilibrium function $\mathbf{r}(s)$ by a variational principle involving the elastic-energy

density given by equation (6), in the particular case $\mathcal{E}_0(\dot{\mathbf{r}}^2) = \frac{1}{2}m\dot{\mathbf{r}}^2$. One arrives easily to the equilibrium fourth-order differential equation:

$$m\ddot{\mathbf{r}} - A\ddot{\mathbf{r}} = \nabla \cdot V(\mathbf{r}), \quad (14)$$

One obtains in a similar way the equilibrium equations for $\mathbf{r}(s)$ and $\mathbf{u}(s)$ from the "new" elastic-energy density:

$$m\ddot{\mathbf{r}} + iA\lambda\ddot{\mathbf{u}} = \nabla \cdot V(\mathbf{r}) \quad \mathbf{u} = \frac{i}{\lambda}\dot{\mathbf{r}}. \quad (15)$$

II. THE TRANSFER MATRIX AND THE ASSOCIATED EFFECTIVE HAMILTONIAN.

A. The Mathematical Construction

The partition function involving the auxiliary variables \mathbf{u}_n together with the effective monomer coordinates \mathbf{r}_n can be easily obtained from the effective elastic density (13):

$$Z = \int \prod_{n=1}^{N-1} d^2\mathbf{r}_n d^2\mathbf{u}_n \exp -b(K_0(\mathbf{r}_{n+1} - \mathbf{r}_n, \mathbf{u}_{n+1} - \mathbf{u}_n) + U(\mathbf{r}_n, \mathbf{u}_n)), \quad (16)$$

where the "kinetic term" $K_0(\mathbf{r}_{n+1} - \mathbf{r}_n, \mathbf{u}_{n+1} - \mathbf{u}_n)$ is given by:

$$K_0(\mathbf{r}_{n+1} - \mathbf{r}_n, \mathbf{u}_{n+1} - \mathbf{u}_n) = \mathcal{E}_0\left(\frac{(\mathbf{r}_{n+1} - \mathbf{r}_n)^2}{b^2}\right) - \frac{(\mathbf{r}_{n+1} - \mathbf{r}_n)}{b} \cdot \mathbf{f} + \frac{i\lambda A}{b^2}(\mathbf{r}_{n+1} - \mathbf{r}_n) \cdot (\mathbf{u}_{n+1} - \mathbf{u}_n), \quad (17)$$

and the total potential $U(\mathbf{r}_n, \mathbf{u}_n)$ by:

$$U(\mathbf{r}_n, \mathbf{u}_n) = V(\mathbf{r}_n) + \frac{A\lambda^2\mathbf{u}_n^2}{2}. \quad (18)$$

It is convenient to define the intermediate partition function $Z_n(\mathbf{r}_n, \mathbf{u}_n)$ associated with a chain having a crystallographic length $s_n = b n$. It obeys the well-known recurrence relation involving the transfer matrix $T(\mathbf{r}_{n+1}, \mathbf{u}_{n+1} | \mathbf{r}_n, \mathbf{u}_n)$:

$$Z_{n+1}(\mathbf{r}_{n+1}, \mathbf{u}_{n+1}) = \int \int d^3\mathbf{r}_n d^3\mathbf{u}_n T(\mathbf{r}_{n+1}, \mathbf{u}_{n+1} | \mathbf{r}_n, \mathbf{u}_n) Z_n(\mathbf{r}_n, \mathbf{u}_n). \quad (19)$$

We introduce the transfer operator \hat{T} associated with the transfer matrix and isolate its "kinetic" part by writing:

$$\hat{T} = \exp -\frac{b}{2}\hat{U} \hat{T}_0 \exp -\frac{b}{2}\hat{U}, \quad (20)$$

$$\langle \mathbf{r}_{n+1}, \mathbf{u}_{n+1} | \hat{T}_0 | \mathbf{r}_n, \mathbf{u}_n \rangle = \exp -b K_0(\mathbf{r}_{n+1} - \mathbf{r}_n, \mathbf{u}_{n+1} - \mathbf{u}_n), \quad (21)$$

where \hat{U} is the operator associated with the potential $U(\mathbf{r}_n, \mathbf{u}_n)$ and $K_0(\mathbf{r}_{n+1} - \mathbf{r}_n, \mathbf{u}_{n+1} - \mathbf{u}_n)$ the "kinetic" elastic-density term given by eq.(17). We note that the free transfer operator \hat{T}_0 is invariant upon space translation. It is then natural to work within a Fourier space basis:

$$\langle \mathbf{k}_{n+1}, \mathbf{q}_{n+1} | \hat{T}_0 | \mathbf{k}_n, \mathbf{q}_n \rangle = (2\pi)^6 \delta^3(\mathbf{k}_{n+1} - \mathbf{k}_n) \delta^3(\mathbf{q}_{n+1} - \mathbf{q}_n) \widetilde{T}_0(\mathbf{k}_n, \mathbf{q}_n), \quad (22)$$

$$\widetilde{T}_0(\mathbf{k}_n, \mathbf{q}_n) = (2\pi)^3 \frac{1}{A\lambda} \exp -b \left(\mathcal{E}_0\left(\frac{\mathbf{q}^2}{A\lambda}\right) + \frac{\mathbf{q}}{A\lambda} \cdot (i\mathbf{k} - \mathbf{f}) \right). \quad (23)$$

We have now all we need to write \hat{T}_0 as the exponential of an Hamiltonian operator \hat{H}_0 symmetric but non-Hermitian. Returning to the ordinary space and introducing the momentum operators: $\hat{\mathbf{p}}_r = -i\nabla_r$ and $\hat{\mathbf{p}}_u = -i\nabla_u$ we get $\hat{T}_0 = \exp(-b\hat{H}_0)$ with \hat{H}_0 given, up to an irrelevant additive constant, by:

$$\hat{H}_0 = \mathcal{E}_0\left(\frac{\hat{\mathbf{p}}_u^2}{A\lambda}\right) + \frac{\hat{\mathbf{p}}_u}{A\lambda} \cdot (i\hat{\mathbf{p}}_r - \mathbf{f}). \quad (24)$$

One sees that eq.(14) is recovered immediately by eliminating \mathbf{u} from the two above equations. Note also that the above expression of \mathbf{u} is just the saddle point relative to the Gaussian integral appearing in the right hand side of the basic identity (10).

The transfer operator \hat{T} defined by equation (22) can be similarly written as: $\hat{T} = \exp(-b \hat{H})$. The total Hamiltonian \hat{H} is readily obtained, up to corrections of order b^2 :

$$\hat{H} = \hat{H}_0 + \hat{U} = \mathcal{E}_0\left(\frac{\hat{\mathbf{p}}_u}{A\lambda}\right)^2 + \frac{\hat{\mathbf{p}}_u}{A\lambda} \cdot (i\hat{\mathbf{p}}_r - \mathbf{f}) + V(\mathbf{r}) + A\frac{\lambda^2}{2}\mathbf{u}^2. \quad (25)$$

B. Physical Interpretation of the Results

In the above derivation of \hat{H}_0 , the auxilliary variable \mathbf{u} and its conjugate momentum \mathbf{p}_u have been introduced in a rather formal way. We would like to stress that the operator $\hat{\mathbf{p}}_u/(A\lambda)$ has a well defined physical interpretation. The fact that it replaces $\dot{\mathbf{r}}$ in going from \mathcal{E}_{new} to \hat{H} , suggests that these two quantities are connected. To make this connection more explicit it is convenient to introduce the "Heisenberg" operator $\hat{r}_i(s) = \exp(s \hat{H}) r_i \exp(-s \hat{H})$, which is commonly used to compute the correlation function $C_{i,j}(s_1, s_2)$ from the formula :

$$C_{i,j}(s_1, s_2) = \text{Tr} \left((\exp -L \hat{H}) \hat{r}_i(s_1) \hat{r}_j(s_2) \right) \text{Tr} \left(\exp -L \hat{H} \right). \quad (26)$$

Let us now compute the s-derivative of $\hat{r}_i(s)$:

$$\hat{v}_i(s) = \frac{d \hat{r}_i(s)}{d s} = \exp(s \hat{H}) [\hat{H}, r_i] \exp(-s \hat{H}) = \frac{\hat{p}_{u_i}(s)}{A\lambda}. \quad (27)$$

In conclusion, the operator $\hat{\mathbf{p}}_u(A\lambda)$ is just the "velocity operator" $\hat{\mathbf{v}} = [\hat{H}, \mathbf{r}]$. In all the explicit computations to be performed later, we shall use a basis diagonal with respect to the velocity operator $\hat{\mathbf{v}}$. Then, the final expression of the Hamiltonian \hat{H} reads:

$$\hat{H}(\mathbf{v}) = -\frac{1}{2A} \nabla_{\mathbf{v}}^2 + \mathcal{E}_0(\mathbf{v}^2) + \mathbf{v} \cdot (\nabla_{\mathbf{r}} - \mathbf{f}) + V(\mathbf{r}), \quad (28)$$

where the real vector \mathbf{v} stands for an eigenvalue of the vector operator $\hat{\mathbf{v}} = \frac{1}{A\lambda} \mathbf{p}_u$. One notes that the "gauge" constant λ has disappeared from the Hamiltonian $\hat{H}(\mathbf{v})$ since all mathematical objects involved have now well defined physical interpretations.

Before applying our formalism to the extension of the WLC model, we have found judicious to try it out on a soluble one-dimensional model. This test will be presented in a separate publication [12].

III. THE EXTENDED WORM LIKE CHAIN MODEL

A. The Extended WLC Hamiltonian.

In order to apply the present formalism to the WLC model with spatial constraints we have to find out the adequate functional form for $\mathcal{E}_0(\mathbf{v}^2)$. The solution is rather simple: one introduces the small length δb such that $\delta b/b \ll 1$ and takes for $\mathcal{E}_0(\mathbf{v}^2)$ the following expression:

$$\mathcal{E}_0(\mathbf{v}^2) = b \frac{(\mathbf{v}^2 - 1)^2}{2\delta b^2}. \quad (29)$$

Using our final expression for the Hamiltonian \hat{H} given by equation (28) together with the above choice of $\mathcal{E}_0(\mathbf{v}^2)$, we get the Hamiltonian $\hat{H}(\mathbf{v}, \delta b)$, from which we shall obtain our extented version of the WLC model by taking the limit $\delta b/b \ll 1$:

$$\hat{H}(\mathbf{v}, \delta b) = -\frac{1}{2A} \nabla_{\mathbf{v}}^2 + b \frac{(\mathbf{v}^2 - 1)^2}{2\delta b^2} + \mathbf{v} \cdot (\nabla_{\mathbf{r}} - \mathbf{f}) + V(\mathbf{r}). \quad (30)$$

Performing the trace upon $v = |\mathbf{v}|$ in the transfer operator $\exp -b \hat{H}(\mathbf{v}, \delta b)$, only the value $v = 1$ does contribute in the limit $\delta b \rightarrow 0$, so that \mathbf{v} coincides with the unitary tangent vector \mathbf{t} appearing in the WLC model. We arrive in this way to *our final Extended WLC (EWLC) Hamiltonian*:

$$\hat{H}_{EWLC} = -\frac{1}{2A} \nabla_{\mathbf{t}}^2 - \mathbf{f} \cdot \mathbf{t} + \mathbf{t} \cdot \nabla_{\mathbf{r}} + V(\mathbf{r}) = \hat{H}_{WLC}(\mathbf{f}) + \mathbf{t} \cdot \nabla_{\mathbf{r}} + V(\mathbf{r}). \quad (31)$$

When $V(\mathbf{r}) = 0$ it is easily seen that the term $\mathbf{t} \cdot \nabla_{\mathbf{r}} = i\mathbf{t} \cdot \hat{\mathbf{p}}_r$ disappears when ones perfoms the trace with respect to \mathbf{r} of the transfer matrix, which is diagonal in the Fourier space. Indeed in such a case, the \mathbf{r} -trace operation is equivalent to taking the limit $\mathbf{p}_r \rightarrow 0$ and the WLC model Hamiltonian is recovered.

B. Solving the EWLC model by the transfer matrix method.

Although it is in principle possible to get the partition function by solving the eigenvalue problem $\hat{H}_{EWLC} \Psi_n(\mathbf{r}, \mathbf{p}) = E_n \Psi_n(\mathbf{r}, \mathbf{p})$ as a partial differential equation with well-defined boundary conditions, we have found both numerically efficient and physically illuminating to work within the transfer matrix formalism. Let us first introduce the WLC model transfer operator $\hat{T}_{WLC}(\mathbf{f}) = \exp -b \hat{H}_{WLC}(\mathbf{f})$ and write down its matrix element for later use:

$$\langle \mathbf{t}_{n+1} | \hat{T}_{WLC}(\mathbf{f}) | \mathbf{t}_n \rangle = \exp -b \left(\frac{A(\mathbf{t}_{n+1} - \mathbf{t}_n)^2}{2b^2} - \frac{1}{2} \mathbf{f} \cdot (\mathbf{t}_{n+1} + \mathbf{t}_n) \right). \quad (32)$$

To proceed, we write the EWLC Hamiltonian \hat{H}_{EWLC} under the following compact form:

$$\hat{H}_{EWLC} = \hat{H}_{WLC}(\mathbf{f} - i \hat{\mathbf{p}}_r) + V(\mathbf{r}); \quad (33)$$

and the EWLC transfer operator \hat{T}_{EWLC} reads:

$$\hat{T}_{EWLC} = \exp -b \frac{V(\mathbf{r})}{2} \exp -\left(\hat{H}_{WLC}(\mathbf{f} - i \hat{\mathbf{p}}_r) \right) \exp -b \frac{V(\mathbf{r})}{2}. \quad (34)$$

The recurrence relation obeyed by the partition function $Z_n(\mathbf{r}_n, \mathbf{t}_n)$ is then given by the following expression:

$$Z_{n+1}(\mathbf{r}_{n+1}, \mathbf{t}_{n+1}) = \int \int d^3 \mathbf{r}_n d^3 \mathbf{t}_n \exp -b \frac{V(\mathbf{r}_{n+1}) + V(\mathbf{r}_n)}{2} \langle \mathbf{r}_{n+1}, \mathbf{u}_{n+1} | \hat{T}_{WLC}(\mathbf{f} - i \hat{\mathbf{p}}_r) | \mathbf{r}_n, \mathbf{u}_n \rangle Z_n(\mathbf{r}_n, \mathbf{t}_n). \quad (35)$$

Let us first evaluate the matrix element of $\hat{T}_{WLC}(\mathbf{f} - i \hat{\mathbf{p}}_r)$, which is diagonal in the momentum basis. The corresponding diagonal element is just the WLC-model transfer matrix given in equation (32) for the case of a complex force $\mathbf{f} - i \hat{\mathbf{p}}_r$. We get in this way an intermediate expression of the $\hat{T}_{WLC}(\mathbf{f} - i \hat{\mathbf{p}}_r)$ matrix element in coordinate space, written as a Fourier integral:

$$\langle \mathbf{r}_{n+1}, \mathbf{t}_{n+1} | \hat{T}_{WLC}(\mathbf{f} - i \hat{\mathbf{p}}_r) | \mathbf{r}_n, \mathbf{t}_n \rangle = \int d^3 \mathbf{p}_r \exp i \mathbf{p}_r \cdot \left(\mathbf{r}_n - \mathbf{r}_{n+1} + b \frac{\mathbf{t}_{n+1} + \mathbf{t}_n}{2} \right) \langle \mathbf{t}_{n+1} | \hat{T}_{WLC}(\mathbf{f}) | \mathbf{t}_n \rangle.$$

Performing the integration over \mathbf{p}_r , a Dirac δ function appears which has a rather transparent physical interpretation:

$$\langle \mathbf{r}_{n+1}, \mathbf{t}_{n+1} | \hat{T}_{WLC}(\mathbf{f} - i \hat{\mathbf{p}}_r) | \mathbf{r}_n, \mathbf{t}_n \rangle = \delta^3 \left(\mathbf{r}_{n+1} - \mathbf{r}_n - b \frac{\mathbf{t}_{n+1} + \mathbf{t}_n}{2} \right) \langle \mathbf{t}_{n+1} | \hat{T}_{WLC}(\mathbf{f}) | \mathbf{t}_n \rangle.$$

We arrive immediately to an expression for the partition-function recurrence relation, where the integration over \mathbf{r}_n has disappeared:

$$\begin{aligned} Z_{n+1}(\mathbf{r}_{n+1}, \mathbf{t}_{n+1}) &= \exp -\frac{b}{2} V(\mathbf{r}_{n+1}) \int d^3 \mathbf{t}_n \exp -\frac{b}{2} V \left(\mathbf{r}_{n+1} - \frac{b}{2} (\mathbf{t}_{n+1} + \mathbf{t}_n) \right) \\ &\quad \langle \mathbf{t}_{n+1} | \hat{T}_{WLC}(\mathbf{f}) | \mathbf{t}_n \rangle Z_n \left(\mathbf{r}_{n+1} - \frac{b}{2} (\mathbf{t}_{n+1} + \mathbf{t}_n) \right). \end{aligned} \quad (36)$$

In order to get a further simplification of the above formula, we shall assume that the rates of variation with $|\mathbf{r}|$ both of the potential $V(\mathbf{r})$ and the starting partition function $Z_0(\mathbf{r}, \mathbf{t})$ are at most of the order of the inverse of the persistence length A , which is assumed much larger than the length b of the elementary link. As a consequence the same property will hold also for $Z_n(\mathbf{r}_n, \mathbf{t}_n)$. This will allow us to make two important simplifications:

1. The two Boltzmann factors involving the potential $V(\mathbf{r})$ can be replaced by a single one, namely: $\exp -b V(\mathbf{r}_{n+1})$.
2. Let us introduce the new set of monomer coordinates: $\mathbf{R}_{n+1} = \mathbf{R}_n + b \mathbf{t}_{n+1}$ with $\mathbf{R}_0 = \mathbf{r}_0$. The relation with the set $\{\mathbf{r}_n\}$ is readily obtained: $\mathbf{R}_n = \mathbf{r}_n + b(\mathbf{t}_n - \mathbf{t}_0)/2$. The assumed rates of variation of $V(\mathbf{r})$ and $Z_0(\mathbf{r})$ imply that the error introduced in the Boltzmann factor and $Z_n(\mathbf{r}_n, \mathbf{t}_n)$ by the replacement $\mathbf{r}_n \rightarrow \mathbf{R}_n$ are of the order of b/A .

By implementing the simplifications 1. and 2. in equation (36) we arrive to our final simplified expression for the partition function recurrence relation which can be regarded as *our definition of the EWLC model*:

$$Z_{n+1}(\mathbf{r}_{n+1}, \mathbf{t}_{n+1}) = \exp -b V(\mathbf{r}_{n+1}) \int d^3 \mathbf{t}_n \langle \mathbf{t}_{n+1} | \hat{T}_{WLC}(\mathbf{f}) | \mathbf{t}_n \rangle Z_n(\mathbf{r}_{n+1} - b \mathbf{t}_{n+1}, \mathbf{t}_n). \quad (37)$$

The physical interpretation of the iteration process is now clearly exhibited and can be given a nice interpretation in terms of a Markovian random walk model in three dimensions. The $(n+1)^{th}$ step is given by $b \mathbf{t}_{n+1}$; its length is b and its direction, defined by the unitary vector \mathbf{t}_{n+1} , is correlated to that of the previous step \mathbf{t}_n through the correlation function $C(\mathbf{t}_{n+1}, \mathbf{t}_n) \propto \langle \mathbf{t}_{n+1} | \hat{T}_{WLC}(\mathbf{f}) | \mathbf{t}_n \rangle$. Within our unit conventions, the "potential" $V(\mathbf{r})$ stands for a potential energy by unit molecular length, written in thermal units, so that $\Delta W_{n+1} = k_B T b V(\mathbf{r}_{n+1})$ represents the amount of energy to be spent or gained by performing the $(n+1)^{th}$ step. The exponential in front of the r.h.s of equation (37) is just the associated Boltzmann factor.

IV. APPLICATION OF THE EXTENDED WLC MODEL TO THE STRETCHING OF DSDNA MOLECULE CONFINED BETWEEN TWO PARALLEL PLATES.

In this section we shall apply our iterative version (eq. 37) of the Extended WLC model to the confinement of a single dsDNA molecule between two parallel plates - called hereafter Plate 1 and Plate 2 - separated by a distance L_0 . One molecular end is anchored upon Plate 1. The other end is attached, for instance, to a magnetic bead pulled by a magnetic tweezer. We do not pretend here to describe a fully realistic situation since, for the sake of simplicity, we shall ignore the spatial constraints associated with the finite dimensions of the magnetic bead. A more complete analysis could be done within our formalism but it falls well outside the introductory scope of this paper. The stretching force is assumed to be normal to the two plates and is pulling away the molecular end from the anchoring plate. The dimensions of the plates normal to the force, measured from the anchoring point, are assumed to be much larger than L_0 and will be considered as infinite. Two physical configurations have been considered.

1. L_0 is supposed to be larger than the crystallographic length L . In our explicit computations we have taken $L_0 = 40 \text{ \AA}$ and $L = 12 \text{ \AA}$. It means that even for large stretching forces the molecular end stays far away from Plate 2. This will allow us to study the deviations of the elongation from the WLC model prediction due to the presence of the anchoring plate (Plate 1), provided we ignore the spatial obstruction of the pulling device.
2. The crystallographic length L is larger than L_0 , so that for large forces the fully stretched molecule cannot fit within the plates. We have studied within our EWLC Model how the molecule adapts itself to this confined situation when the elongation predicted by the WLC Model reaches values larger

than $L_0 = 20 \text{ \AA}$.

A. Basic formulae for the two-plate confinement configurations .

Our confinement configurations are clearly invariant under rotations around the z -axis defined by the anchoring point and the stretching force direction and therefore

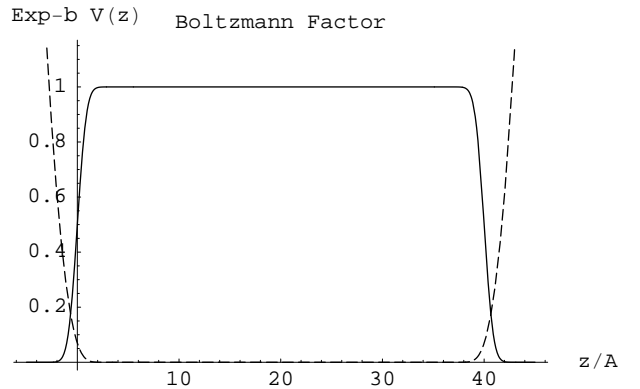


FIG. 1: We have displayed in this figure the two-plate confining potential $V(z)$ (dotted line), together with the associated Boltzmann factor $\exp -b V(z)$ (full line). $b = A/10$ is the elementary link length. The Boltzmann factor is given explicitly as the product of two rounded-off step functions $\Theta(z, \Delta z) \Theta(L_0 - z, \Delta z)$ with a smoothing length $\Delta z = A$ and $L_0 = 40 \text{ \AA}$ is the two-plate distance.

the partition function $Z_n(\mathbf{r}_n, \mathbf{t}_n)$ depends only upon two *independent* variables z_n and θ_n : z_n is the z -axis component of the n^{th} monomer coordinate \mathbf{r}_n and $\cos \theta_n$ is the projection of the tangent vector \mathbf{t}_n upon the z -axis. As a consequence, the partition function obeys the recurrence relation which is easily deduced from equation (37) by performing an average around the z -axis:

$$Z_{n+1}(z_{n+1}, \theta_{n+1}) = \exp -b V(z_{n+1}) \int_0^\pi d\theta_n \sin \theta_n T_{WLC}(\theta_{n+1}, \theta_n, f) Z_n(z_{n+1} - b \cos \theta_{n+1}, \theta_n). \quad (38)$$

The azimuthal-averaged WLC transfer matrix can be obtained by taking the zero torque limit of the corresponding

expression given in ref.[11] for the supercoiled DNA case:

$$T_{WLC}(\theta_1, \theta_2, f) = \exp -\left\{ \frac{A}{b} (1 - \cos \theta_1 \cos \theta_2) + \frac{bf}{2} (\cos \theta_1 + \cos \theta_2) \right\} \times I_0\left(\frac{A \sin \theta_1 \sin \theta_2}{b}\right). \quad (39)$$

In order to get a potential $V(z)$ simulating the two confining plates satisfying the smoothness condition at the persistence-length scale, it is convenient to introduce the rounded off step function:

$$\Theta(z, \Delta z) = \frac{1}{2} + \frac{1}{2} \operatorname{erf}(z/\Delta z), \quad (40)$$

where $\operatorname{erf}(x)$ is the “error” function : $\frac{2}{\sqrt{\pi}} \int_0^x \exp -t^2 dt$ and Δz the smoothing length assumed to be $\sim A$. Instead of the potential $V(z)$, it is more convenient to write directly the Boltzman factor :

$$\text{Boltz}(z, L_0, \Delta z) = \exp -b V(z) = \Theta(z, \Delta z) \Theta(L_0 - z, \Delta z). \quad (41)$$

Its variation with respect to the reduced variable z/A is represented by the solid curve of Figure 1 for $\Delta z = A$. The dotted curve gives the variation of the external potential associated with an elementary link $b V(z_n)$.

The next point to be specified is the initial condition of our recurrence procedure. A detailed analysis of the anchoring mechanism at the microscopic level being beyond the scope of this paper, we have adopted a prescription which incorporates in a simple way some features of the actual physical situation. We choose as the molecular chain origin ($n = 0$) the end of the initial strand sticking out from the anchoring plate and having a length $\sim A$. The initial partition function $Z_0(z_0, \theta_0)$ is written as follows :

$$Z_0(z_0, \theta_0) = \frac{1}{2\sqrt{2\pi}\sigma} \exp -\frac{1}{2}(z_0/\sigma)^2. \quad (42)$$

A look at the potential $V(z)$ on Figure 1. shows that z_0 can take negative as well as positive values within the range $(-A, A)$, so that a Gaussian centered curve looks quite realistic if $\sigma \sim A$. Similarly the tangent-vector z -axis projection $\cos \theta_0$ lies within the interval $(-1, 1)$ so that a $\cos \theta_0$ uniform distribution seems an acceptable guess. We note, finally, that our choice of $Z_0(z_0, \theta_0)$ satisfies the smoothness condition assumed in the previous section. The $n = 1$ partition function $Z_1(z_1, \theta_1)$ is then readily obtained by plugging $Z_0(z_0, \theta_0)$ in the r.h.s. of the recurrence relation (38).

We would like to give now a few indications about the numerical methods we have used in the transfer matrix iteration.

In order to perform the integral over θ_n we use the following discretization procedure. We divide the variation interval $0 \leq \theta_n \leq \pi$ into n_s segments $\frac{(s-1)\pi}{n_s} \leq \theta_n \leq \frac{s\pi}{n_s}$. The integral over each segment is done with the standard Gauss method involving n_g abscissae and n_g attached

weights. The integral over the full θ_n interval is then approximated by a discrete weighted sum over $d = n_s n_g$ points:

$$\int_0^\pi f(\theta_n) \sin \theta_n d\theta_n = \sum_{i=1}^d w_i \sin \theta_i f(\theta_i).$$

The transfer-matrix iteration involves a z variable translation $z_n \rightarrow z_{n+1} - b \cos \theta_{n+1}$ to be performed upon $Z_n(z_n, \theta_n)$ for each value $\theta_n = \theta_i$. This is achieved by building at each step the interpolating function $Z_{n,int}(z, \theta_i)$ associated with the array: $\{z_l = z_{min} + l b, Z_n(z_l, \theta_i)\}$ with $1 \leq l \leq n_{max}$. An appropriate choice of n_{max} leads to a physically relevant sample of the monomer coordinates throughout the iteration process.

For more extensive computations than those presented in this paper, one should consider a potentially more efficient method involving the Fast Fourier Transform (FFT) algorithm. It is based upon the remark that a variable translation performed upon a given function reduces to a phase shift upon its Fourier transform: $\tilde{Z}(p, \theta_i) \rightarrow \exp -ib \cos \theta_i \tilde{Z}(p, \theta_i)$. An inverse FFT will then be required to perform the multiplication by the Boltzmann factor.

B. Modification of the elongation-versus-force curve induced by the anchoring plate barrier.

We would like to present here the result of a numerical simulation based upon the iteration process built up from the recurrence relation given in eq. (38). Our aim was to study the barrier effect of the anchoring plate (Plate 1.) upon the elongation-versus-force curve. This corresponds to the configuration 1, introduced previously, where the distance between the plates L_0 is larger than the cristallographic length L . The values used in our simulation are $L_0 = 40$ \AA and $L = 12$ \AA . It is, then, clear that Plate 2 plays no role since we have decided to ignore the eventual presence of a magnetic bead attached to the molecule free end. At each step n we store the normalized probability distribution $P_n(z_n, \alpha)$ where $\alpha = FA/(k_B T)$ is the reduced force parameter. We have plotted in Figure 2 the relative molecular elongation $\langle z \rangle / L = \int dz z_N P_N(z_N, \alpha) / L$ versus α , where $N = L/b$. The dotted curve represents the prediction of the standard WLC model which assumes that the anchoring device reduces to a point. The full curve corresponds to the elongation-versus-force obtained in our simulation within the EWLC model; it exhibits clearly the anchoring-plate barrier effect which leads to a relative elongation of 34% in the zero force limit. For higher forces, the two curves

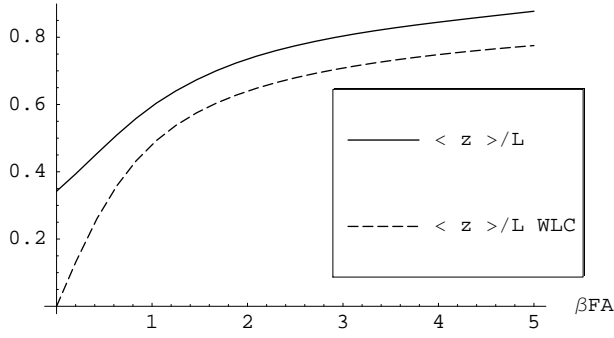


FIG. 2: This figure illustrates the effects of the anchoring plate barrier upon the elongation-versus-force curve. The upper curve (full line) gives the prediction of the EWLC model when $L/A = 12$. The other plate is lying at a distance $L_0 = 10 L/3$ and, as a consequence, has no effect upon the elongation. The fact that the elongation curve is pushed upward with respect to the unconstrained WLC prediction (dotted curve) has a simple qualitative explanation: because of the anchoring plate barrier the $z < 0$ half space is not accessible to the nucleotides whatever the stretching force.

become approximately parallel with an offset of about 10%. It is possible to get from our simulation an expansion in powers of $\sqrt{A/L}$ at fixed force, giving the upward elongation displacement $\Delta_{bar}\langle z/L \rangle$ induced by the anchoring plate barrier. As an illustration, we give the result for two typical forces corresponding to $\alpha = 0$ and $\alpha = 1$. We found that the second-order expansion, $\Delta_{bar}\langle z/L \rangle = a_1(\alpha)\sqrt{\frac{A}{L}} + a_2(\alpha)\frac{A}{L}$, gives a very good fit to our simulation data within the range: $5 \text{ \AA} \leq L \leq 30 \text{ \AA}$. For $\alpha = 0$ we get: $a_1(0) = 1.00$ $a_2(0) = 0.65$. The large value of $a_1(0)$ can be interpreted in terms of an hemispheric molecular cluster around the anchoring point with a radius growing like \sqrt{N} . The results look rather different when $\alpha = 1$: $a_1(1) = -0.06$ $a_2(1) = 1.57$. The strong decrease of the $\sqrt{\frac{A}{L}}$ coefficient - confirmed by the $\alpha = 2$ results - seems to suggest that the anchoring plate barrier affects a fixed number of monomers when $\alpha \geq 1$.

C. Flattening of the stretched molecule against Plate 2 when the cristallographic length is larger than the two-plate distance.

This section is devoted to the analysis of the simulation results obtained for the configuration 2: a molecular chain having a cristallographic length $L = 30 \text{ \AA}$ is confined between two plates separated by a distance $L_0 = 20 \text{ \AA}$. The stretching force is specified by taking the value $\alpha = F A/(k_B T) = 5$ for the reduced force parameter. The unconstrained WLC model would lead to a relative elongation $\langle z \rangle / L = .775$, to be compared with the ratio $L_0/L = 2/3 \simeq 0.667$. It follows that a molecule stretched according to the WLC model prediction could not fit inside the plates.

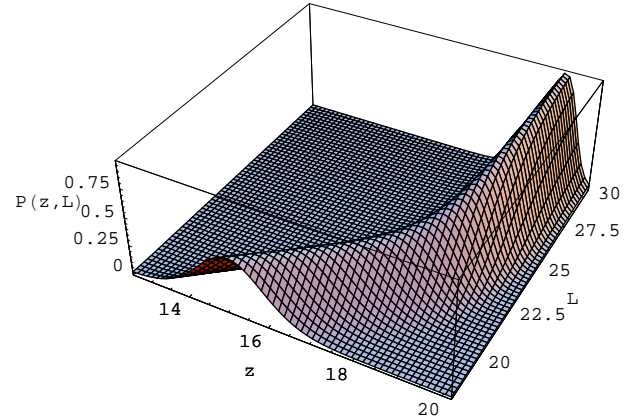


FIG. 3: The 3 D plot displayed in this figure gives the probability distribution of the coordinate z of the molecule end when the cristallographic length L varies from $0.9 L_0$ to $1.5 L_0$ with $L_0 = 20 \text{ \AA}$. In our simulation we have taken a stretching force such that the elongation predicted by the unconstrained WLC model is $\langle z \rangle = 1.16 L_0$ when L takes its maximum value. It is then clear that such a molecule, stretched according to the usual WLC model, could not fit between the plates. When L approaches its maximum value $1.5 L_0$ the elongation $\langle z \rangle$ is no longer increasing like L but tends to its maximum possible value L_0 ; at the same time the slope of the hill is becoming steeper and this indicates a decrease of the longitudinal fluctuations of the chain. This clearly suggests that the end part of the molecular chain is getting flattened against the neighbouring plate.

Our iteration procedure provides us with the end point distributions $P(L, z)$ for various molecular lengths $L \leq 30 \text{ \AA}$. At each step we store the probability $P_n(z(n))$ and by identifying $L = n b$ we build the discrete set: $P(L/b, z) = P_n(z)$. The probability distribution $P(L, z)$ is then obtained by interpolation. We have displayed in Figure 3 a 3D plot of $P(L, z)$. It allows us to follow in a continuous way how the DNA molecule manages to satisfy the two-plate space constraints. When $18 \leq L \leq 20$ the molecule does not feel yet the Plate 2 barrier and the hill ridge, projected upon the (L, z) plane, follows a straight line with a slope $\Delta z / \Delta N$ given by the standard WLC model. When L enters the domain $20 \leq L \leq 30$ the ridge bends under the barrier repulsion to become parallel to the plates. At the same time the hill slope becomes steeper under the combined effect of the stretching force and the confining plates. So we have a clear evidence for the *flattening of the molecular chain against Plate 2*.

In Figure 4 we have presented the results of a quantitative analysis of the confinement effects we have just described in a qualitative way.

Our first result, plotted on the solid line curve, gives the thermal average of the projection of the tangent t_n along the z axis, $\cos\theta(n) = b^{-1}(z(n) - z(n-1))$, when $15 \text{ \AA} \leq n b = L \leq 30 \text{ \AA}$. It is easily obtained from the probability $P_n(z)$ using the following equation:

$$\langle \cos\theta(n) \rangle = \frac{1}{b} \int dz z (P_n(z) - P_{n-1}(z)) \quad (43)$$

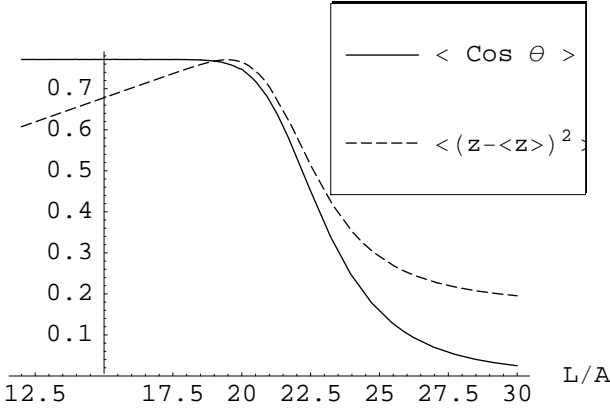


FIG. 4: This figure contains two plots which exhibit, in a quantitative way, the features already visible on Figure 3. The dotted curve gives the variations of the longitudinal fluctuations of the molecular chain $\Delta z^2 = \langle (z - \langle z \rangle)^2 \rangle$ when the crystallographic length L varies within the interval $(3/4 L_0, 3/2 L_0)$. When $3/4 L_0 < L < L_0$, Δz^2 grows like L as predicted by the unconstrained WLC model and then starts to decrease when $L > L_0$. The full line curve gives the thermal average $\langle \cos \theta \rangle$ of the projection of the end-point tangent vector upon the z axis (the symmetry axis of the problem). When $L < L_0$, $\langle \cos \theta \rangle$ is independent of L and the height of the plateau is given by the relative elongation predicted by the unconstrained WLC model. When $L > L_0$, $\langle \cos \theta \rangle$ begins to fall sharply towards 0. These two combined effects suggest that the molecular end follows, around the symmetry axis, a zigzagging path, which tends to become parallel to the neighbouring plate when $L \rightarrow L_{max} = 3/2 L_0$.

Let us take, for example $L = 30 A = n_{end} b$, and follow the variation of $\langle \cos \theta(n) \rangle$ when the effective monomer number n varies between $n = 15 A/b = 150$ and $n_{end} = 300$. If n stays within the range $150 \leq n \leq 200$ the average $\langle \cos \theta(n) \rangle$ has a constant value given by the WLC model. (The height of the plateau agrees within a few tenths of a percent with the exact WLC prediction quoted above.) This confirms the previous conclusion that for $L < 20 A$ the molecular entropic elasticity is not affected by the Plate 2 barrier. For $n > 200$ a new feature appears: $\langle \cos \theta(n) \rangle$ decreases continuously to reach the value close to 0 for $n = n_{end}$. This suggests that the molecular chain starts to follow a zigzagging path around the z axis (the symmetry axis of the problem), the zigzags becoming nearly parallel to the neighbouring plate when n approaches its maximum value n_{end} . One might argue that another way to explain why $\langle \cos \theta(n) \rangle \rightarrow 0$ when $n \rightarrow n_{end}$ would be to assume that the zigzags are along the z axis like in the case of an elastic ball bouncing back and forth against a plate. However it is easily seen that this cannot be the dominant mechanism. First, the entropy of a one-dimensional zigzagging path is much smaller than a two-dimensional one. Furthermore the bouncing ball picture implies an increase of the fluctuation of $z(n)$. This contradicts our prediction for $\Delta z^2(n) = \langle (z(n) - \langle z(n) \rangle)^2 \rangle$ displayed on Figure 4 (dot-

ted curve). For $n < 200$, $\Delta z^2(n)$ increases linearly with n as predicted by the WLC model but starts a rather sharp decrease for $n > 200$, as this is also apparent on our 3D graph.

V. SUMMARY AND CONCLUSION

In this paper we have built an extension of the WLC (EWLC) model in order to provide a simple way to implement local spatial constraints upon dsDNA. They are represented by a potential $V(\mathbf{r})$ acting upon the effective monomer with coordinate \mathbf{r} , associated with the coarse-grained molecular chain. In the usual WLC formulation, the molecular contour line is described by the unitary tangent vector $\mathbf{t}(s) = d\mathbf{r}(s)/ds$. Unfortunately this leads to very awkward expressions for the potential energies. The answer to this problem is obvious: use as dynamical variable the monomer $\mathbf{r}(s)$ coordinate ! However, a price has to be paid: the curvature term $\frac{1}{2}A\ddot{\mathbf{r}}_n^2$ introduces a second-order derivative in the elastic-energy linear density and the analogy with a Quantum Mechanics problem used in reference [8] is now harder to establish.

The strategy we have followed to deal with this problem is to eliminate the second-order derivative in the elastic-energy density by introducing an appropriate auxiliary vector variable \mathbf{u} . The procedure has been applied to the class of models defined by the linear energy density: $\mathcal{E}(s) = \mathcal{E}_0(\dot{\mathbf{r}}^2) + \frac{1}{2}A\ddot{\mathbf{r}}^2 - \mathbf{f} \cdot \dot{\mathbf{r}} + V(\mathbf{r})$. Our starting point is a simple identity involving a Gaussian integral. With some simple manipulations, we arrive to a new energy linear density which depends only upon the first derivatives $\dot{\mathbf{r}}(s)$ and $\ddot{\mathbf{u}}(s)$. Then, we go through the usual construction of the Hamiltonian operator \hat{H} from a functional integral giving the partition function. This allows us to use the Quantum Mechanics techniques of ref.[8]. The auxiliary variable \mathbf{u} is defined up to an arbitrary multiplicative constant λ . By making an appropriate choice of λ , we were able to identify its conjugate momentum operator \hat{p}_u to the “velocity operator” $\hat{\mathbf{v}} = [\hat{H}, \mathbf{r}]$. When \hat{H} is written in a basis diagonal with respect to $\hat{\mathbf{v}}$, it takes a remarkably simple form (See eq. (28). The application of this result to the WLC model is rather straightforward: one has to choose $\mathcal{E}_0(\mathbf{v}^2) = b(\mathbf{v}^2 - 1)^2/(2\delta b^2)$. By taking the limit $\delta b/b \ll 1$, one can identify \mathbf{v} to the unitary vector \mathbf{t} of the WLC model. We arrive finally to the rather remarkable relation between our EWLC model Hamiltonian and the WLC model one:

$$\hat{H}_{EWLC} = \hat{H}_{WLC}(\mathbf{f}) + \mathbf{t} \cdot \nabla_{\mathbf{r}} + V(\mathbf{r}).$$

The reaction of some people in front of this formula was sometimes to say: “that’s too simple to be true !”. This is why, besides the fact we have not been able to find a convincing hand-waving argument, we have gone through a detailed - but rather heavy - derivation.

Instead of trying to get the partition function by solving the eigenvalue problem relative to the differential op-

erator \hat{H}_{EWLC} , as it was done in ref. [8] for the unconstrained WLC model, we have found physically more illuminating and numerically more efficient to follow an iterative construction procedure based upon the transfer matrix formalism. We have introduced the n^{th} -order partition function $Z_n(\mathbf{r}_n, \mathbf{t}_n)$, giving the probability distribution of the variables \mathbf{r} and \mathbf{u} relative to the n^{th} effective monomer of the discretized molecular chain. This function obeys a recurrence relation involving only the first nearest neighbour. Starting from the transfer operator $\hat{T} = \exp -b \hat{H}_{EWLC}$, we arrived with some algebra and the help of two mild technical assumptions to the recurrence relation, which we believe constitutes *the most intuitive formulation of our EWLC model*:

$$Z_{n+1}(\mathbf{r}_{n+1}, \mathbf{t}_{n+1}) = \exp -b V(\mathbf{r}_{n+1}) \times \int d^3 \mathbf{t}_n \langle \mathbf{t}_{n+1} | \hat{T}_{WLC}(\mathbf{f}) | \mathbf{t}_n \rangle Z_n(\mathbf{r}_{n+1} - b \mathbf{t}_{n+1}, \mathbf{t}_n).$$

The above iterative construction of the polymer can be viewed as a Markovian random walk in 3 dimensions. The $(n+1)^{th}$ step $\Delta \mathbf{r}_{n+1} = b \mathbf{t}_{n+1}$ is correlated to the previous one through the transfer matrix \hat{T}_{WLC} of the standard WLC model. At each step a certain amount of potential energy, positive or negative, is exchanged with the thermal bath. This transaction probability is governed by the Boltzmann factor sitting in front of the r.h.s of the recurrence formula.

As an illustration of the formalism developed in this paper, we have analysed the configurations of a dsDNA molecule, having a crystallographic length L and confined between two parallel plates separated by a distance L_0 . One molecule extremity is attached by a biochemical binding to one plate. The other molecule end is subject to a constant stretching force normal to the plates, which is pulling away the molecule from the anchoring plate. Our theoretical description is not totally realistic since we have ignored, for the sake of simplicity, the spatial obstructions caused by the stretching device (magnetic or optical tweezers). Despite its limitation, which might be overcome by a more elaborate treatment, our analysis has exhibited rather significant confinement effects which might be relevant to more realistic configurations.

Our first analysis deals with the situation where $L/L_0 = 0.3$. It is clear that only the anchoring plate barrier plays a role, whatever the value of the pulling force. We have found that the elongation-versus-force curve is pushed upward with respect to the WLC prediction (see Figure 2). This was to be expected since the anchoring-plate barrier prevents the monomers to make incursions into the $z \leq 0$ half-space. In the zero force limit, the relative elongation goes to a finite value: 0.35 when $L = 12 \text{ \AA}$. For higher forces specified by $\alpha = F A / (k_B T) \geq 1$ the two elongation curves tend to become parallel with an offset $\simeq 0.1$. We have studied the upward relative elongation shift as a function of $\sqrt{A/L}$ within the range: $5 \leq A/L \leq 30$. In the zero force limit the absolute elongation shift is found approximately equal to $\sqrt{A/L}$. This

suggests the presence around the anchoring point of a molecular hemispheric cluster growing like \sqrt{N} , while for higher forces we found that the anchoring barrier affects only a fixed number of monomers.

Our second simulation concerns a confined situation which occurs when the dsDNA molecule has a crystallographic length $L = 30 \text{ \AA}$ larger than the two-plate separation $L_0 = 20 \text{ \AA}$. Our computations were done for a reduced force parameter $\alpha = 5$. The standard WLC model predicts a relative elongation equal to 0.775, a number significantly larger than the ratio $L_0/L = 2/3$. In other words, the dsDNA molecule, stretched according to the standard WLC model, cannot fit within the plates. Our aim was to follow continuously how a molecule with a variable length L manages to satisfy the two-plate constraints when L varies from $L_{min} = 15 \text{ \AA}$ to $L_{max} = 30 \text{ \AA}$. In Figure 4 we have displayed a 3 D plot giving the probability distribution $P(z, L)$ of the end point z , for a given L . For $L < 20 \text{ \AA}$, no problem, the molecule follows the WLC predictions up to a fixed offset. When $L > 20 \text{ \AA}$, there is a gradual flattening of the molecular chain against the neighbouring plate, accompanied by a decrease of the z fluctuations. Another significant feature concerns the thermal average of the end point tangent vector projected upon the z axis, $\langle \cos \theta \rangle$. It remains locked to the WLC value 0.77 when $L \leq 18 \text{ \AA}$ and then decreases continuously when $L > 18 \text{ \AA}$ towards a value close to 0 when L reaches the value $L_{max} = 30 \text{ \AA}$. Together with the sharp decrease of the z fluctuations, this suggests that the molecule follows around the z axis (symmetry axis of the problem) a zigzagging path which becomes gradually parallel to the plates.

We would like to suggest, among others, two possible applications of the theoretical tools presented in this paper.

- In references [9, 10, 11] the WLC model has been generalized to a Rod Like Chain (RLC) Model, involving both bending and twisting rigidities. This makes possible the study of supercoiled dsDNA entropic elasticity below the denaturation threshold. One can easily extend the RLC model in order to incorporate spatial constraints. The recurrence relation for the partition function $Z_n(z_n, \theta_n, \kappa)$ relative to a supercoiled DNA molecule, with a given torque $\Gamma = k_B T \kappa$ acting upon its free end, is obtained by performing in the recurrence relation r.h.s. the following replacement:

$T_{WLC}(\theta_{n+1}, \theta_n, f) \rightarrow T_{RLC}(\theta_{n+1}, \theta_n, f, -\kappa^2)$, where T_{RLC} is given explicitly in ref.[11]. The anchoring-plate barrier is expected to have significant effects upon the so-called “hat curves”, giving, for a given force, the relative elongation versus the supercoiling reduced parameter σ . Taking, for example, the “low” force case, $F \simeq 0.1 \text{ pN}$, the RLC model “hat curve” dips steeply into the negative z region when $|\sigma| \geq 0.03$. This effect, which can be accounted for by plectonem-like structures, is totally suppressed by the anchoring-plate barrier.

- Although the analysis of dsDNA entropic-elasticity data [8] seems to suggest that self-avoiding corrections to the WLC model are not very important, this is not the case for supercoiled dsDNA. Marko and Vologodskii have found using Monte-Carlo simulations [13] that the “hat curves” are significantly modified when $|\sigma| \geq 0.04$. We would like to point out that the extended RLC model sketched above suggests a possible approach to self-avoiding effects which would have been totally intractable within the original WLC or RLC model. It is well known that the polymer self-avoidance generated by a monomer-monomer repulsive potential $V(\mathbf{r}_1, \mathbf{r}_2)$ can be mapped into the problem of a polymer interacting with a one-monomer imaginary stochastic potential $i\phi(\mathbf{r})$. The functional probability measure of $\phi(\mathbf{r})$ is of the Gaussian type and specified by the two-field product av-

erage $\langle \phi(\mathbf{r}_1, \phi(\mathbf{r}_2)) \rangle_\phi = V(\mathbf{r}_1, \mathbf{r}_2)$ [14]. This problem is now amenable to Quantum Field Theory techniques, but it remains to be seen if a useful approximation scheme can be devised, using the fact that dsDNA is a remarkably stiff polymer.

Acknowledgments

It is a pleasure to thank D. Bensimon, M.-A. Bouchiat and J. Iliopoulos for their careful reading of this manuscript and valuable suggestions.

Laboratoire de Physique Théorique de l’Ecole Normale Supérieure is a Unité Mixte du Centre National de la Recherche Scientifique et de l’Ecole Normale Supérieure (UMR 8549).

[1] C. Bustamante, Z. Bryant and S. Smith, *Nature* **421**, 423-427 (2003).
[2] J.F Allemand, D Bensimon and V. Croquette, *Curr. Op. Structural Biology* **13**, 266-274 (2003).
[3] S.B. Smith, L. Finzi and C. Bustamante, *Science* **258**, 1122 (1992).
[4] T.T. Perkins, S.R. Quake, D.E. Smith and S. Chu, *Science* **264**, 8222 (1994).
[5] T.R. Strick, J.-F. Allemand, D. Bensimon, A. Bensimon and V. Croquette, *Science* **271**, 1835 (1996).
[6] M. Fixman and J. Kovac, *J. Chem. Phys.* **58**, 1564 (1973).
[7] J.F. Marko and E.D. Siggia, *Science* **265**, 506 (1994).
[8] C. Bouchiat, M.D. Wang, S.M. Block, J.-F. Allemand and V. Croquette, *Biophys. J.* **76**, 409 (1999).
[9] C. Bouchiat and M. Mézard, *Phys. Rev. Lett.* **80**, 1556 (1998).
[10] For an analytic perturbation treatment of supercoiled dsDNA in the high force limit see: J.D Moroz and P. Nelson, *Proc. Natl. Acad. Sci. USA* **94**, 11418 (1997), *Macromolecules* **3**, 6333 (1998).
[11] C. Bouchiat and M. Mézard, *Eur. Phys. J.E.* **2**, 377-402 (2000).
[12] C. Bouchiat, in preparation.
[13] J.F Marko and A.V. Vologodskii, *Biophys. J.* **78**, 123 (1997).
[14] G. Parisi, *Statistical Field Theory* in Advanced Book Classics (1998), Perseus Books.
[15] This term can be estimated to be of the order of $1/N$ compared to the integral contribution, within the extended WLC model to be discussed later on.